https://doi.org/10.5194/tc-2023-127
Preprint. Discussion started: 25 August 2023

The Cryosphere Discussions
Open Access EGU

Snow Water Equivalent Retrieval Over Idaho, Part B: Using L-band UAVSAR Repeat-Pass Interferometry

Zachary Hoppinen[*1,2], Shadi Oveisgharan[3], Hans-Peter Marshall[1], Ross Mower[4,5], Kelly Elder[6], and Carrie Vuyovich[7]

[1]Boise State University, Department of Geosciences, 1295 University Drive, Boise, ID, USA
[2]Cold Regions Research and Engineering Laboratory, Engineer Research and Development Center, United States Army, Hanover, NH 03755, USA
[3]Jet Propulsion Laboratory, California Institute of Technology, 4800 Oak Grove Dr, Pasadena, CA, USA
[4]The National Center for Atmospheric Research, Boulder, Colorado, USA.
[5]Department of Civil and Environmental Engineering, University of Washington, Seattle, WA, USA
[6]Rocky Mountain Research Station, US Forest Service, Fort Collins, CO, USA
[7]Hydrological Sciences Laboratory, NASA Goddard Space Flight Center, Greenbelt, MD, USA

Correspondence: Zachary Hoppinen (Zachary.Keskinen@boisestate.edu)

Abstract. This study evaluates using interferometry on low frequency synthetic aperture radar (SAR) images to monitor snow water equivalent (SWE) over seasonal and synoptic scales. We retrieved SWE changes from nine pairs of SAR images, mean 8 days temporal baseline, captured by an L-band aerial platform, NASA's UAVSAR, over central Idaho as part of the NASA SnowEx 2020 and 2021 campaigns. The retrieved SWE changes were compared against coincident in situ measurements (SNOTEL and snow pits from the SnowEx field campaign) and to 100 m gridded SnowModel modeled SWE changes. The comparison of in situ to retrieved shows a strong Pearson correlation (R = 0.80) and low RMSE (0.1 m, n = 64) for snow depth change and similar results for SWE change (RMSE = 0.04 m, R = 0.52, n = 57). The comparison between retrieved SWE changes to SnowModel SWE change also showed good correlation (R = 0.60, RMSD = 0.023 m, n = 3.2e6) and especially high correlation for a subset of pixels with no modeled melt and low tree coverage (R = 0.72, RMSD = 0.013 m, n = 6.5e4). Finally, we bin the retrievals for a variety of factors and show decreasing correlation between the modeled and retrieved values for lower elevations, higher incidence angles, higher tree percentages and heights, and greater cumulative melt. This study builds on previous interferometry work by using a full winter season time series of L-band SAR images over a large spatial extent to evaluate the accuracy of SWE change retrievals against both in situ and modeled results and the controlling factors of the retrieval accuracy.

1 Introduction

Seasonal snow is a critical resource providing drinking water for millions, clean hydro-electric power generation, and supporting multi-billion dollar agricultural and recreation industries, with the total value of seasonal snow estimated in the trillions of dollars (Li et al. , 2017; Sturm et al. , 2017). Consequently, understanding the distribution of seasonal snow water storage and subsequent runoff is essential.

https://doi.org/10.5194/tc-2023-127
Preprint. Discussion started: 25 August 2023

Current techniques fail to effectively resolve snow properties for water forecasters and managers in the face of a changing global climate that will fundamentally alter previous relationships between snowpack monitoring sites (SNOTEL), point-based automatic weather stations and runoff forecasts. Climate change will bring shifts in the timing and intensity of melt rates (Kunkel , 2016), more frequent rain-on-snow events (Cohen , 2015), and complex region-specific evolution in snowfall patterns (Strapazzon et al. , 2021; Domingues et al. , 2012). These changes are altering the relationship between point observations (e.g. SNOTEL sites) and snow conditions at other elevations, and therefore the statistical techniques for using sparse in-situ snow measurements to predict spring run-off are becoming less accurate (Livneh and Badger , 2020). A shift to spatially distributed snow estimates is required, however due to the short length scale of variability in snow, increasing the in-situ network to the necessary station density is not logistically or economically feasible. Remote sensing and modeling represent a promising method of determining spatially distributed snow estimates to capture the complexities of snow distributions. Remote sensing of snow water storage currently relies primarily on passive-microwave systems with coarse tens of kilometer-scale resolution. Additionally, passive microwave systems can only measure snow depths up to a meter and; therefore, are not valuable for mountainous areas where most of the water available for water resource usage is stored. Active microwave-based synthetic aperture radar (SAR) does not have depth limitations or resolution constraints making it useful for measuring and resolving complex global snow water storage patterns.

1.1 SAR overview

SAR sensors actively emit electromagnetic energy in the microwave range, frequencies from 1 to 40 GHz, and measure the backscattered (returning) energy and phase. For lower frequency, longer wavelength microwave SAR systems over snow-covered ground, the electromagnetic waves are refracted across the air-snow interface and then reflected from the snow-ground interface with limited snow grain interactions. Passing through the snowpack leads to two competing effects: shorter two-way travel distance but slower wave speeds. These effects combine to create phase shifts, due to the changes in travel time, between repeat SAR images that we can analyze to quantify snow height and snow water equivalent changes (Figure 1). Analyzing phase changes between SAR images, called interferometric SAR (InSAR), allows us to retrieve changes in the snowpack volume using these SAR-observed snow height changes and modeled or observed densities.

Since the returned phases are measurements of sinusoidal wave offsets there is a "wrapping" effect where as the phase approaches and then passes 2π it returns to zero again. This causes an 2π modulo ambiguity that has be resolved by unwrapping the phase and adding or subtracting increments of 2π to the phase to recover the absolute or unwrapped phase. This unwrapping process is relatively simple in high coherence regions but may be impossible in lower coherence regions. Consequently, InSAR analysis may use either the wrapped phase, when continuous data is required and the expected phase change is less than 2π, or unwrapped data when the expected phase change may exceed 2π.

In this study, we use Equation 1, proposed by Guneriussen et al. (2001), to retrieve snow height changes (Δd) at a specific wavelength (λ) from incidence angle (α), phase change ($\Delta\phi$), and the real component of the dielectric permittivity (ϵ_s). ϵ_s measures the wave speed through the snowpack and depends on only the snowpack density and liquid water content. We

https://doi.org/10.5194/tc-2023-127
Preprint. Discussion started: 25 August 2023

The Cryosphere Discussions

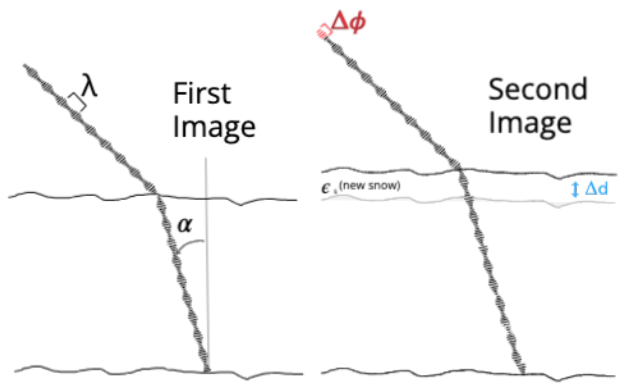

Figure 1. Conceptual model of phase differences between two SAR images with an increase in snow height between image acquisitions. Δd is the increase in snow height between the first and second images, $\Delta\phi$ is the corresponding shift in phase due to changes in path length and wave speed, α is the incidence angle, λ is the wavelength, and ϵ_s is the real-component of the dielectric constant of the new snow.

estimated the real component of the dielectric permittivity from snowpack density (ρ_s) in kg m^{-3} using Equation 2, assuming no liquid water in the snowpack (Matzler , 1996).

$$\Delta d = -\frac{\Delta\phi\lambda}{4\pi}\frac{1}{\cos\alpha - \sqrt{\epsilon_s - \sin^2\alpha}} \quad (1)$$

$$\epsilon_s = 1 + 1.6\times10^{-3} * \rho_s + 1.8\times10^{-9} * \rho_s^3 \quad (2)$$

InSAR retrievals of the amount of water stored in the snowpack, snow water equivalent (SWE), are generally preferred to capturing snow height changes for two reasons. First, most water managers are primarily interested in the volume of water stored within the snowpack rather than the height of snow. Secondly, conversion to SWE should minimize the effects of errors in the estimation of ρ_s in Equation 2. For example, an overestimation of ρ_s will lead to a slower estimated wave speed through the snowpack and an underestimation of snow depth. However, when we convert the retrieved snow depth to SWE using this higher density, this underestimation of depth is counteracted, minimizing the impact of errors in density. For this analysis we directly use our density estimates from the inversion to snow depth to convert retrieved snow depth to snow water equivalent.

1.2 Previous work

Previous research has demonstrated promising retrievals of snow height and SWE changes using InSAR phase shifts in seasonal mountain snowpacks. However, these studies have focused on simple topography with limited numbers of InSAR pairs and have yet to explore the accuracy or controlling factors of InSAR retrievals in complex mountain terrain (Marshall et al. , 2021; Deeb et al. , 2011).

https://doi.org/10.5194/tc-2023-127
Preprint. Discussion started: 25 August 2023

The Cryosphere Discussions

Guneriussen et al. (2001) showed fringe patterns consistent with snow accumulation in a pair of March ERS-1, C-band ($\lambda \approx 0.05$ m), images that captured a 4 centimeters change in SWE but did not have in situ observations to validate the change. Marshall et al. (2021) explored L-band, ($\lambda \approx 0.231$ m), snow depth inversion over a 4-km ^{2} region on Grand Mesa, Colorado, using lidar and UAVSAR imagery from February 1 and February 12, 2020, and showed good agreement between lidar depth change and UAVSAR estimated depth change (r^2=0.76, RMSE $<$ 0.05 m). Tarricone et al. (2022) used three L-band InSAR pairs to estimate both accumulation and ablation in the Jemez River, New Mexico, with accumulation and ablation patterns showing agreement with both in-situ depth sensors and changes in fractional snow covered area. Ruiz et al. (2021) successfully captured a season-long SWE accumulation at a tower-based site using InSAR phase changes at L-band with temporal baselines up to 12 days in length at L-band. Comparison to in situ SWE showed RMSEs between 8.77-26.07 mm depending on the temporal baseline used in the analysis. Additionally, they showed an overestimation of SWE by 7-21 mm of SWE from the tower-based L-band InSAR compared to the in situ SWE measurements. Finally, Nagler et al. (2022) measured SWE changes using a C and L-band airborne InSAR instrument for a pair of snowfall events. The in situ measurements captured 66.4 mm of SWE change, and the L-band InSAR captured a mean SWE change of 70.3 mm with a root mean squared difference of 11.2 mm. These studies demonstrate the promise of InSAR SWE and depth retrievals at both C and L-band. We expand on these previous studies by increasing the number of in situ observations and image pairs analyzed and utilizing the large study areas which include complex topography and a large elevation range to explore controlling factors on the accuracy of InSAR retrievals.

1.3 Research questions

We explore two research questions to clarify the ability of lower frequency, L-band radars to retrieve snow properties:

1. How accurate are snow depth and SWE change retrievals over complex mountain terrain using L-band interferometric radar analysis?
2. How does tree coverage, total snow depth, incidence angle, coherence, and snow wetness impact the accuracy of L-band interferometric retrievals?

2 Methods

2.1 Datasets

This research combines in situ, modeled, and aerial data sets of snow properties over the central mountains of Idaho to address our research questions (Figure 2). We use the weekly to biweekly time series of L-band SAR observations from UAVSAR collected for the 2020 and 2021 NASA SnowEx Mission, to retrieve snow depth and SWE. The validation data included in situ observation from weekly snow pits (depth, SWE, wetness), telemetered snow station measurements, interval boards (Greene et al. , 2022) and spatially distributed model results of both SWE and SWE melt. Additionally, we explored how the retrieval accuracy changed with vegetation and topography, using geomorphological and vegetation data from the 10-m USGS National

https://doi.org/10.5194/tc-2023-127
Preprint. Discussion started: 25 August 2023

Table 1. UAVSAR Flight Dates

Flight 1 Date	Flight 2 Date	Unwrapped?
2019-12-20	2020-01-31	N
2020-01-31	2020-02-13	N
2020-02-13	2020-02-21	Y
2020-02-21	2020-03-11	Y
2021-01-15	2021-01-20	Y
2021-01-20	2021-01-27	Y
2021-01-27	2021-02-03	Y
2021-02-03	2021-02-10	Y
2021-02-10	2021-03-03	N
2021-03-03	2021-03-10	Y
2021-03-10	2021-03-16	Y
2021-03-16	2021-03-22	Y

Elevation Dataset (NED) (Gesch et al. , 2018), 2016 National Land Cover Database 30-m vegetation percentage maps (Jin et al. , 2019) and 2019 30-m Global Land Analysis and Discovery forest height dataset (Potapov et al. , 2021).

2.2 UAVSAR imagery

The UAVSAR platform is a fully polarimetric L-band InSAR instrument mounted on a NASA Gulf Stream III aircraft (Hensley , 2008; Rosen et al. , 2006), and was tasked to perform weekly to bi-weekly observations over 14 sites in the Western U.S. from January to March for the 2020 and 2021 Nasa SnowEx Mission. The UAVSAR imagery was processed by the NASA Jet Propulsion Laboratory, including SAR focusing and georeferencing with the Shuttle Radar Topography Mission (SRTM) DEM, radiometric calibration, motion compensation, and phase unwrapping using the Integrated Correlation and Unwrapping (ICU) algorithm (Rosen et al. , 2006; Fore et al. , 2015). The imagery was downloaded and converted to netCDFs using *uavsar_pytools* (Hoppinen et al. , 2022).

This study used 12 UAVSAR image pairs from the 2019-2020 and 2020-2021 winters over central Idaho from repeated flight paths at a heading of 232° (Table 1). These image pairs were all nearest temporal neighbors from 14 image acquisitions. We utilized only the nine image pairs that successfully unwrapped for most analyses. We utilized the wrapped images when complete spatial or temporal coverage was necessary and explicitly state that when appropriate below. The bounding box for these images was ≈170 x 16 km and stretched from the foothills of Boise into the Sawtooth Mountains. This box includes Dry Creek Experimental Watershed, Mores Creek Summit, and Banner Summit, where field teams performed in situ observations on the flight dates (Figure 2).

https://doi.org/10.5194/tc-2023-127
Preprint. Discussion started: 25 August 2023

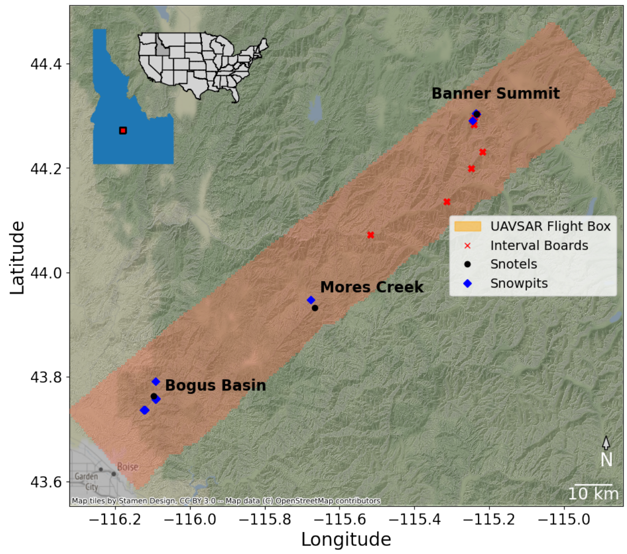

Figure 2. Map of the study area showing the locations of the UAVSAR flight box, snow pits, and SNOTEL locations.

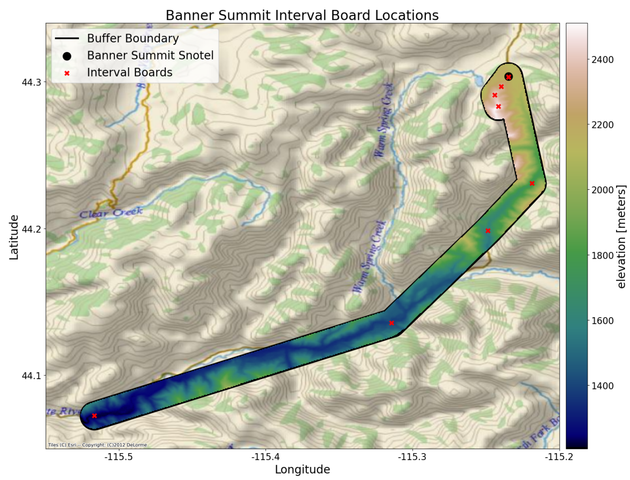

Figure 3. Map of the interval board locations and the buffer around sites used to clip the UAVSAR data.

2.3 In Situ Observations

The in situ data included automated weather station data from SNOTEL stations, SWE increase measurements from interval boards, and snow pits coincident with UAVSAR flights from the Dry Creek, Mores Creek, and Banner Creek study sites. Interval board data collected the accumulated snow depth and SWE between UAVSAR flights from 4-9 locations near the Banner summit SNOTEL (Figure 3). The SNOTEL stations used were SNTL:ID:978 (Bogus), SNTL:ID:637 (Mores), and SNTL:ID:312 (Banner) (USDS National Resource Conversation Service , 2022). SNOTEL data used included 2m air temper-

https://doi.org/10.5194/tc-2023-127
Preprint. Discussion started: 25 August 2023

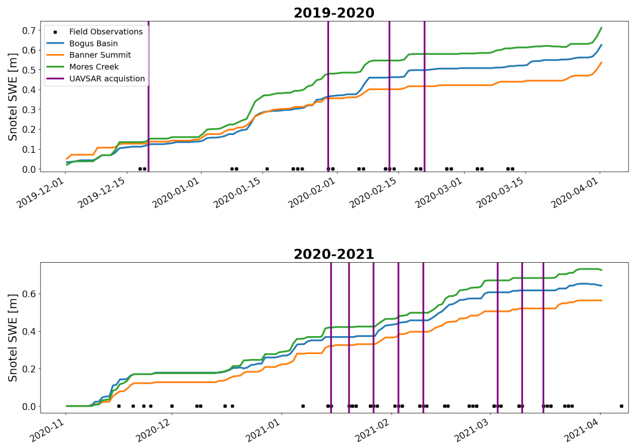

Figure 4. 2020 and 2021 snow water equivalent graphs for the three SNOTELs used in this study. Purple lines represent UAVSAR flights and black xs represent days with field observations.

ature, snow depth, and snow water equivalent at hourly time steps. The snow pit observations included measurements of total snow depth, dielectric permittivity, full density profiles in 10 cm increments, layer-based measurements of snow wetness and grain form, and site descriptions of vegetation and ground cover (Table 2). For each InSAR image pair, repeat snow pits within +/- 2 days of both flights were included (Figure 4).

2.4 SnowModel

A distributed snow-evolution modeling system (SnowModel) can be used to simulate snow properties (e.g., snow depth, SWE, snow melt, snow density, etc.) over different climates and landscapes (Liston and Elder , 2006; Liston et al. , 2020). The SnowModel domain is on a structured grid with spatial resolutions ranging from 1 to 200 meters (although it has the ability to simulate coarser resolutions, as well) and temporal resolutions ranging from 10 minutes to 1 day. The required inputs to run SnowModel include 1) temporally varying meteorological variables of precipitation, wind speed and direction, air temperature, and relative humidity taken from meteorological stations or atmospheric models and 2) spatially distributed topography and land-cover type. The primary modeled processes include accumulation from frozen precipitation; blowing-snow redistribution and sublimation; interception, unloading, and sublimation within forest canopies; snow-density and grain-size evolution; and snowpack ripening and melt (Liston and Elder , 2006).

The modeled daily aggregated SWE and melt data were generated by simulations using Parallel SnowModel, a parallelized version of SnowModel (Mower et al. , 2023). The data was indexed from Parallel SnowModel simulations executed using 1,800 processes on NASA's Center for Climate Simulation (NCCS) Discover supercomputer with a 1,560-teraflop SuperMicro Cluster feature 20,800 Intel Xeon Skylake processes (Carriere , 2023) over the contiguous United States (CONUS) at a 100-meter grid increment with a 3-hour forcing time step, daily aggregated output, and single-layer snowpack configuration. The following inputs were used for the simulations: USGS NED for topography on a 30-meter grid (Gesch et al. , 2018), the North

https://doi.org/10.5194/tc-2023-127
Preprint. Discussion started: 25 August 2023

Table 2. SnowEx snow pits

Site Name	Date Range	Number of Coincident Pairs	Latitude	Longitude
Banner Summit SNOTEL	2020-01-30 - 2021-03-22	12	44.29086	-115.24387
Lower Deer Point - Open	2021-01-21 - 2021-03-23	8	43.73691	-116.12208
Lower Deer Point - Tree	2021-01-21 - 2021-03-23	6	43.73634	-116.12072
Bogus Basin Lower Trees	2021-01-22 - 2021-03-18	5	43.75689	-116.09078
Bogus Basin Lower	2021-01-22 - 2021-03-24	8	43.75705	-116.09099
Mores Creek Summit	2020-02-12 - 2021-03-04	2	43.94735	-115.67666
LDP Open	2020-01-31 - 2020-03-11	4	43.73701	-116.12188
LDP Tree	2020-01-31 - 2020-03-11	4	43.73640	-116.12050
Banner Summit Open	2020-01-30 - 2021-03-18	5	44.30461	-115.23598
Bogus Basin Upper	2020-01-31 - 2020-03-11	4	43.75878	-116.09017

American Land Change Monitoring System (NALCMS) Land Cover 2015 map for vegetation on a 30-meter grid (Homer et al. , 2015; Jin et al. , 2019; Latifovic et al. , 2012), and forcing variables from a high-resolution Weather Research Forecast(WRF) model from the National Center for Atmospheric Research (NCAR) on approximately a 4-kilometer grid (Rasmussen et al. , 2023).

3 InSAR snow depth retrievals

3.1 Polarization

For this analysis, we utilized the phase changes from the VV polarization, based on higher coherence in the co-polarized band than in the cross-polarized bands. The choice of VV over HH was due to higher coherence in VV and to minimize interactions of the radar echos with vegetation and ice layers, which might raise the phase centroid above the ground surface.

https://doi.org/10.5194/tc-2023-127
Preprint. Discussion started: 25 August 2023

The Cryosphere Discussions

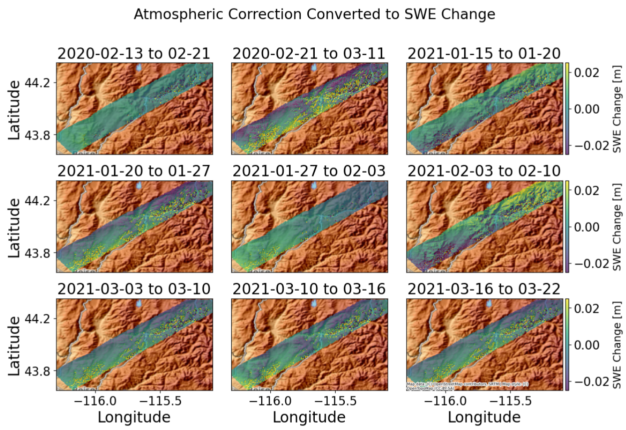

Figure 5. Changes in the retrieved SWE from each time period from atmospheric corrections. Note that each atmospheric correction was normalized to a mean of zero and plotted with the same color bounds to improve comparisons.

3.2 Setting the UAVSAR reference phase

An essential consideration of InSAR imagery is the need for a reference phase. In order to set this reference phase for the in situ analysis, we set the mean phase of each image pair to match the expected phase from the mean snow depth changes from all in situ observations, snotels and snow pits, bracketing the two flights (+/- 2 days). We calculated the mean phase from regions with non-zero modeled SWE to minimize impacts from non-snow related factors. We calculated the phase that would match the mean in situ observed snow depth change using Equation 1, the mean image incidence angle, and mean in situ density. For the model comparison, we set the mean phase of each image pair using the mean modeled phase from the scene-wide change in SWE using the mean in situ density to estimate scene-wide dielectric permittivity, however, note that the SWE retrieval is not very sensitive to density (Leinss et al. , 2015).

3.3 Atmospheric correction

We corrected for atmospheric phase delays due to temporally varying water vapor, air temperatures and pressures by downloading ERA5 atmospheric data for all acquisition dates and calculating the z-integrated phase delay difference between acquisition dates for each pair of images (Hoppinen et al. , 2022; Hersbach et al. , 2020; Doin et al. , 2009). This phase delay difference was then subtracted from the measured InSAR phase changes.

We elected to use a retrospective atmospheric models to remove atmospheric phase instead of phase elevation relationships to avoid removing our SWE accumulation signal which can be correlated with elevation. To visualize the impacts of these atmospheric corrections, we converted these atmospheric corrections to theoretical errors in the SWE retrieval using the incidence angle raster and the mean in situ density for each pair of images (Figure 5).

https://doi.org/10.5194/tc-2023-127
Preprint. Discussion started: 25 August 2023

The Cryosphere Discussions

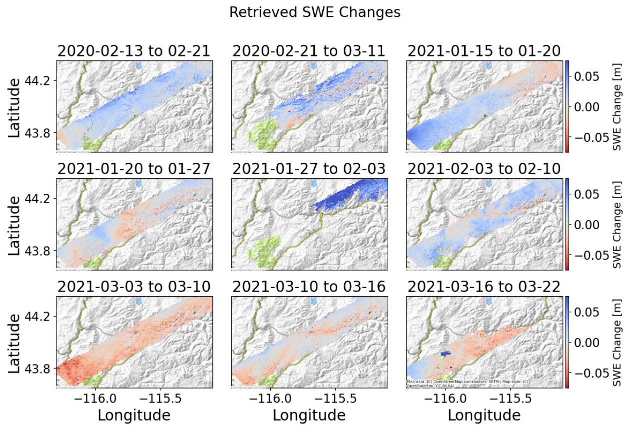

Figure 6. The retrieved SWE change in meters for each pair of nearest neighbor image pairs. To improve comparison these are all plotted on the same color bounds.

3.4 Retrieving SWE changes

For each UAVSAR image pair, we used the mean in situ density from the relevant SNOTEL and snow pit observations to estimate the dielectric permittivity combined with the local incidence angle and phase to calculate the snow depth and SWE change at each pixel using Eq 1 (Figure 6).

4 Statistical comparison of InSAR SWE retrievals

We began by visualizing the SNOTEL SWE and snow depth time series for January 2021 to March 2021 against the retrieved time series from UAVSAR acquisitions. To generate our UAVSAR retrieved snow depth profiles, we used the in situ measured depth and SWE at our first flight date (January 15th, 2021) and then cumulatively added the retrieved mean snow depth or SWE from a 100 m box around the SNOTEL. As some image pairs and regions failed to unwrap (Table 1, Figure 6), we used the wrapped phase to ensure we would be able to retrieve a continuous SWE retrieval time series for all the SNOTEL sites.

We next compared the UAVSAR snow depth and SWE change retrievals to the field snow pits and SNOTELs combined using the Pearson correlation coefficient (r), root mean squared error (RMSE), and mean absolute bias (retrieved - in situ). The retrieved values were averaged from a 100m box around the field location. The snow pits were selected if they were within +/-2 days of either the first or second flight in a pair. We subtracted the snow depth from spatially coincident pits to get the snow depth change observed between flights. We calculated 95% confidence intervals for RMSE, Pearson-r, and bias from one thousand bootstrapped samples of the UAVSAR and in situ snow depth changes (n = 64).

To explore how effectively the UAVSAR-retrieved SWE captured orographic trends in accumulation, we compared the relative increase in SWE from a series of interval boards at varying elevations near the Banner Summit study site to the relative increases in retrieved UAVSAR SWE changes. We set the SWE change to zero at the lowest board and calculated the changes

https://doi.org/10.5194/tc-2023-127
Preprint. Discussion started: 25 August 2023

in SWE change at each elevation we had an interval board. We did the same for the UAVSAR retrieved SWE change within a 1-kilometer buffer around a line connecting the interval board locations. The UAVSAR SWE change in that buffer was then binned by elevation and plotted against the increase in SWE on the interval boards. We used the wrapped phase in this analysis to avoid bias due to aspects or elevations with lower coherence.

We compared the SnowModel and UAVSAR retrieved SWE changes by calculating Pearson-r and root mean squared difference (RMSD) for all pixels, a subset of pixels that had no modeled SWE melt, and another subset of pixels with no modeled melt and with tree percentages below 10%. We chose RMSD over RMSE for the comparison of modeled to retrieved SWE due to the error between the SnowModel and in situ measurement (RMSE = 0.15 m, R = 0.45). Using RMSD better captures that differences between retrieved and modeled results do not necessarily represent primarily errors in the retrieved values but represent some combined and unknown contributions of errors from both datasets. Next, to explore how RMSD changed with varying geophysical and snow properties, we compared the changes in RMSD by plotting the temporal RMSD at each pixel against the temporally averaged coherence, tree percentage, elevation, maximum modeled SWE depths, and average SWE melt. We used the wrapped phases in this comparison step to avoid biasing the results from low-coherence areas that failed to unwrap and since the magnitude of SWE change in our study region rarely exceeds 2π. We then binned the RMSDs across the whole parameter ranges for elevation, incidence angle, tree percentage, tree height, coherence, and cumulative melt. We excluded bins with less than 100 pixels to avoid bias from small sample sizes.

5 Sensitivity analysis

To explore how phase changes relates to snow properties at L-band, we calculated the theoretical phase change across physically reasonable ranges of snow depth change (0 - 0.5 m), new snow density (100 -300 kg m^{-3}), and incidence angles (30-60°) (Figure 7). These results show that phase wrapping should not occur until quite significant snow accumulations of 127 mm of SWE at 30° and 80 mm at 60°.

Liquid water in the snowpack impacts radar's wave speed and phase change and consequently causes errors in retrievals since we only parameterize the dielectric permittivity based on density. We parameterized the dielectric constant for dry and wet snow to evaluate the effect of liquid water. We evaluated the increase in retrieved snow depths with no actual increase for varying degrees of liquid water percentage (Tiuri et al. , 1984). The impacts of liquid water in the snowpack are significant. They can cause up to an $\approx$0.1 m overestimation of new snow accumulation in the retrievals, with only 0.1 meters of snow becoming wet (Figure 8).

6 Results

We compare UAVSAR retrieved SWE and snow depths against SNOTEL SWE and snow depth changes, SWE and snow depth changes from consistently located snow pits, interval board SWE increases, and SnowModel's SWE change.

https://doi.org/10.5194/tc-2023-127
Preprint. Discussion started: 25 August 2023

The Cryosphere Discussions

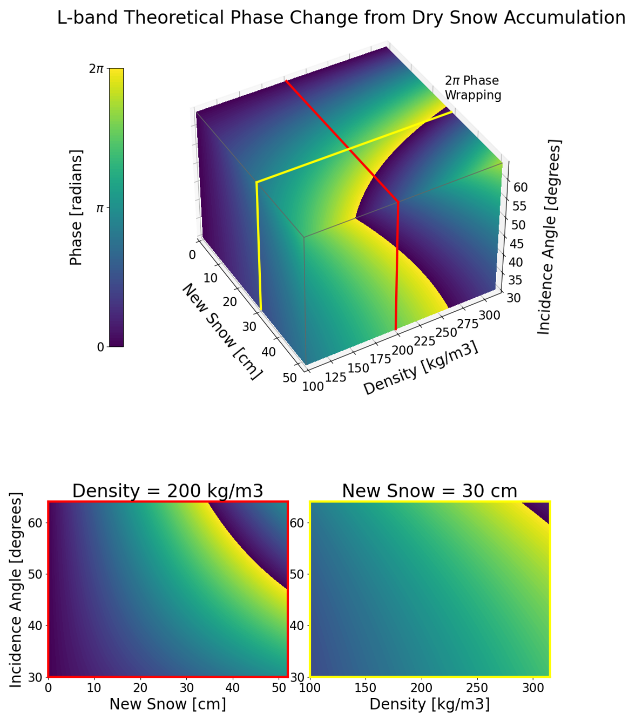

Figure 7. Theoretical phase increases for varying new snow amounts, densities, and incidence angles. The 2π wrapping point data is annotated. Slices through the cube are shown for a constant 200 kg/m^3 density (red, bottom left) and for a constant 30 centimeters of new snow (yellow, bottom right).

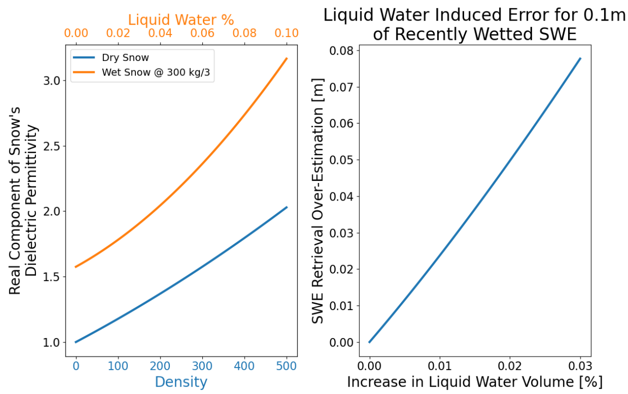

Figure 8. On the left, the theoretical dielectric permittivity for varying snow density (blue) and wetness (orange, constant 300 kg m^{-3} density) using the equations from Tiuri et al. (1984). On the right, SWE retrieval errors caused by 0.1 meters of SWE that increased by varying liquid water percentages in wetness between SAR images.

https://doi.org/10.5194/tc-2023-127
Preprint. Discussion started: 25 August 2023

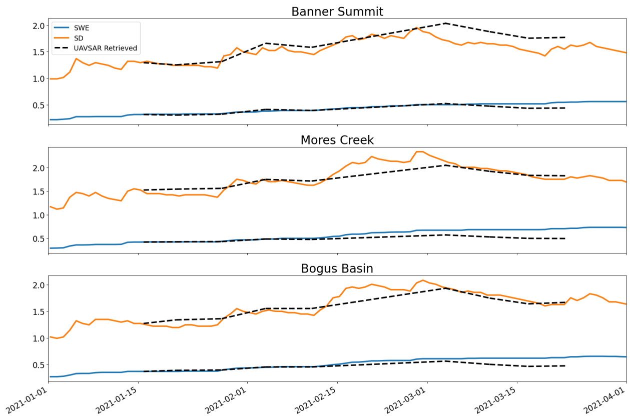

Figure 9. Snotel in situ measured snow depth profile plotted against the cumulative retrieved UAVSAR snow depth changes for a 100 m box around each SNOTEL location. Note that the initial snow depth was set to the in situ measured snow depth at the first flight date in 2021.

6.1 SNOTEL visualization

The time series of snow depth from our three SNOTEL sites matches well against our retrieved UAVSAR time series. Since we had longer temporal separations between our UAVSAR observations, some short temporal scale patterns were missed. Overall, the trends and magnitudes of snow depth accumulation are well captured (Figure 9).

6.2 In situ comparison

An expanded comparison, including snow pit and SNOTEL data, shows a positive agreement between retrieved and in situ snow depth observations with an RMSE of 0.1 m and a Pearson correlation of 0.80 (n = 64)(Figure 10). The bootstrapped analysis had a 95% confidence interval for the RMSE of 0.09 - 0.11 m, with a mean RMSE of 0.10 m, Pearson correlation of 0.71 to 0.87, and bias confidence interval of -0.028 to 0.012 m. The full SWE retrieval were more scattered with an RMSE of 0.041 m and a Pearson correlation of 0.4 (n = 64). Removing in situ retrievals with unreasonably high (> 500 kg m^{-3}) inferred density from the in situ measured SWE and snow depth change improves the RMSE to 0.039 and the Pearson correlation to 0.52 (n = 57).

6.3 Comparison to interval boards

The UAVSAR retrieved SWE changes captured the overall trends in precipitation relative to elevation for most image pairs, with the atmospherically corrected trends in SWE change generally improving the relationship to the measured orographic trends (Figure 11).

https://doi.org/10.5194/tc-2023-127
Preprint. Discussion started: 25 August 2023

The Cryosphere
Discussions
Open Access

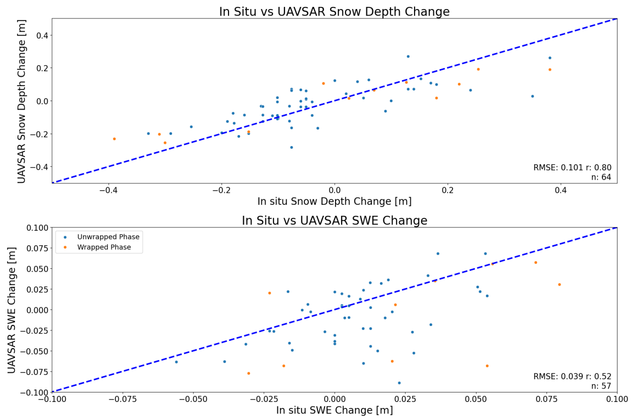

Figure 10. Comparison of the UAVSAR snow depth retrievals to in situ snow depth and SWE change measurements. In situ observations without successful phase unwrapping used the wrapped phase in orange. Note that seven SWE change observations were removed for have measured in situ new snow densities above 500 kg m^{-3}.

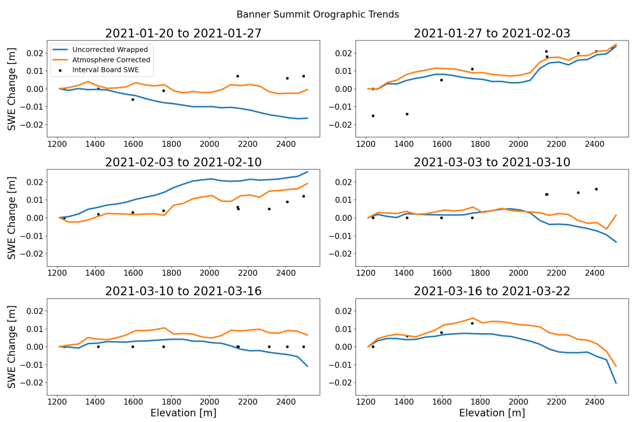

Figure 11. Comparison between the retrieved UAVSAR SWE changes with elevation relative to the interval board data sets on SWE changes with elevation. Note the consistent y-limits for all subplots.

6.4 Comparison to SnowModel

We first qualitatively compared the SnowModel SWE changes to those captured in the phase images for two periods of increasing SWE with successful phase unwrapping near the Banner Summit and the Mores Creek SNOTELs (Figure 12). Both examples showed similar accumulation patterns to SnowModel, but consistently more significant SWE changes in the UAVSAR retrieved SWE changes than SnowModel.

The relationship between the SnowModel and UAVSAR SWE change for all the successfully unwrapped pixels showed large regions of highly negative SWE changes in the retrieved data. However, subsetting to only pixels with no SWE melt

https://doi.org/10.5194/tc-2023-127
Preprint. Discussion started: 25 August 2023

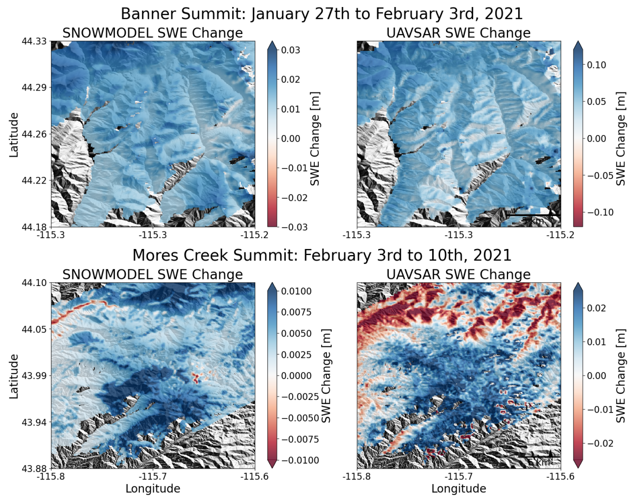

Figure 12. Comparison of the UAVSAR and SnowModel SWE changes for two accumulation periods near the Banner Summit and Mores Creek SNOTELs. Note the different visualization ranges for the SnowModel and UAVSAR SWE changes.

in SnowModel results removed these regions, suggesting that large areas of wet snow were causing bias in the SWE change retrievals (Figure 13).

The spatial maps of RMSD between the SnowModel and retrieved SWE changes show much higher RMSDs at lower elevations along the valley bottoms, in regions to the southeast with higher average SWE melt, and along higher elevations with higher maximum SWE values (Figure 14).

The binned analysis of RMSD generally agreed with the spatial comparison with improving RMSD for higher elevations, steeper incidence angles, lower tree heights and coverage percentage, higher coherences, and lower cumulative melt quantities (Figure 15).

7 Discussion

7.1 How accurate are L-band SWE and snow depth change retrievals over complex mountain terrain?

Our results suggest that L-band InSAR is a promising technique for retrieving snow depth changes over complex mountainous terrain. The comparison between in situ snow depth changes compared to retrieved snow depths show a strong correlation, r = 0.80, and reasonable errors, RMSE = 0.10 m. The comparison to the modeled SWE changes also showed good correlation and low RMSD (RMSD = 0.041 m, r = 0.49). This comparison was even more favorable in dry snow with low tree coverage (RMSD = 0.014 m, r = 0.72). These results suggest that L-band InSAR snow depth change retrievals capture reasonable trends and may be a valuable tool for measuring SWE and snow depth changes.

It is interesting that the retrieved SWE changes compared worse (r = 0.40) relative to the snow depth change (r = 0.80) for the in situ results. This may have been the result of errors in field measurements due to the challenges of measuring SWE

https://doi.org/10.5194/tc-2023-127
Preprint. Discussion started: 25 August 2023

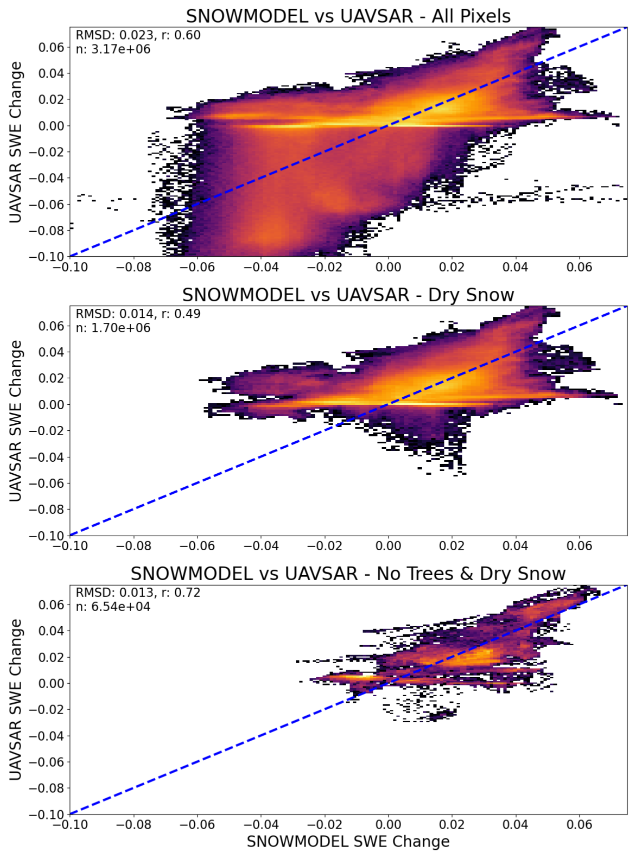

Figure 13. 2D log-scaled heat maps showing UAVSAR vs SnowModel SWE changes for all possible unwrapped pixels (top), subset to only pixels with no modeled melt (middle), and subset to pixels with no modeled melt in regions with less than 20% tree percentage (bottom).

changes in the field relative to measuring snow depth changes. In fact a number of observations had unreasonably high new snow densities (> 500 kg m^{-3}) suggesting either a large rain event or measurement error occurred.

7.2 How do vegetation, incidence angle, slope, and snow-wetness impact the accuracy of L-band retrievals?

The predominant factors in the accuracy of this retrieval technique are the need for dry snow and avoiding high vegetation coverage. The highest RMSDs relative to the modeled data occurred in pixels with high tree cover percentages and large amounts of modeled SWE melt, suggesting that wet snow and vegetation may be negatively effecting retrievals.

The negative impacts on accuracy due to liquid water match our theoretical expectations. Since we parameterize the real component of the snow's dielectric permittivity based solely on density, we expect retrievals of snow depth changes in newly wet snow to diverge from in situ and modeled measurements. This divergence will impact not only the measurements at that specific location but also throw off the mean phase change of the image leading to systemic biases across the image when setting

https://doi.org/10.5194/tc-2023-127
Preprint. Discussion started: 25 August 2023

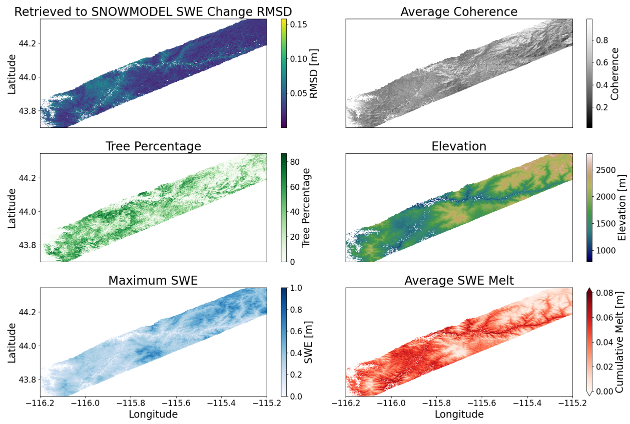

Figure 14. Spatial distribution of the RMSD between the SnowModel and wrapped UAVSAR SWE changes, coherence averaged across all time periods, NLCD tree cover percentage, SRTM elevation, the modeled maximum SWE depth, and average SWE melt across all time periods.

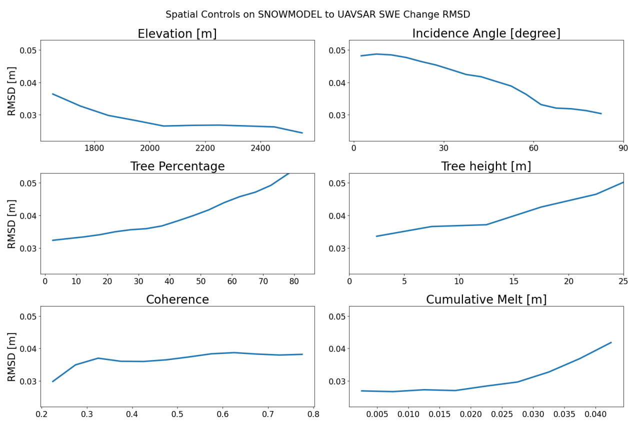

Figure 15. Binned distribution of the RMSD between the SnowModel and wrapped UAVSAR SWE changes, coherence averaged across all time periods, NLCD tree cover percentage, SRTM elevation, the modeled maximum SWE depth, and average SWE melt across all time periods.

the reference phase. Future researchers could improve retrievals by using modeled melt values to improve the parameterization of potentially wet pixels.

The impact of vegetation also matches the theoretical expectation that the increase in scatterers in the vegetation, primarily branches and trunks at L-band, would cause a decrease in the coherence of those pixels due to more random movements of the scatterers within the pixel and a shifting of the phase centroid up towards the above-snow scatterers, breaking our theoretical requirement of a phase centroid at or close to the snow-ground interface. Interestingly Figure 15 showed a minimal relationship between coherence and RMSD above 0.35 m, suggesting that the decrease in coherence might have been a smaller factor.

https://doi.org/10.5194/tc-2023-127
Preprint. Discussion started: 25 August 2023

Alternatively, the model performs worse in the trees, meaning that the increase in RMSE is due to errors in the modeled data rather than UAVSAR retrievals. The lack of a clear relationship in the in situ data between the vegetation classification at the snow pit and retrieval accuracy also suggests that vegetation impacts may be less significant.

The elevation and incidence angle were other factors related to the retrieval accuracy. The impact of elevation is most likely due to its covariance with liquid water in the snowpack and tree coverage in the scene. Incidence angle was negatively correlated with RMSE. Referring to Figure 7, we see that for a constant change in SWE, the induced phase shift is less at lower incidence angles. This decreased phase signal is closer to the instrument noise floor, and we may struggle to capture these small snow depth changes.

7.3 Limitations

This study has a few limitations that should be addressed: the accuracy of SnowModel for comparison and setting the reference phase with the in situ data used for validation.

The SnowModel results used in this analysis showed a reasonable correlation to in situ results (r = 0.45, RMSE: 0.15 m), but errors that we attribute to the InSAR results in Figure 15 (in highly vegetated or wet snow regions) are actually some unknown combination of modeling and InSAR retrieval errors compounding. Future work using either more validated SnowModel results or lidar snow depth retrievals will be necessary and our study's modeling comparison should be interpreted with caution focusing mostly on identifying larger spatial and temporal trends in accumulation.

Another consideration is that we set the reference phase using the average snow depth change and density from across our in situ observations and the average phase of snow-covered regions for each InSAR pair (see "Setting the UAVSAR Reference Phase" section) and then used the same in situ observations for validation. Since we are using the reference phase from the whole image and the average snow change across multiple sites there shouldn't be too much biasing of our results but it is important to know that the calibration and validation data were the same data. We chose to set the reference phase this way due to the limited number of repeat observations available to use and to avoid biasing a whole image from errors in a single in situ measurement, but future work that explores other ways to set the reference phase will be important.

7.4 Future work

Future research and practical applications of InSAR-based SWE retrievals should consider: 1. the importance of atmospheric corrections, 2. how to integrate this technique into pre-existing hydrologic monitoring efforts, 3. effective use of in situ data for processing and validating these InSAR retrievals, 4. image masking in wet and low coherence regions, 5. validating these findings with different snow climates and vegetation profiles, 6. parameterizations for the dielectric permittivity in wet snow, and 7. how best to incorporate other frequencies and SAR-based analysis techniques.

Atmospheric correction of InSAR data to account for temporal and spatial variations in radar wave speeds through the atmosphere due to pressure, temperature, and moisture changes is critical for accurately capturing SWE changes. Due to the relationship between elevation and path length in airborne and spaceborne InSAR systems, the atmospheric phase changes will often have similar patterns to orographic precipitation. This relationship makes the removal of the atmospheric phase critical

https://doi.org/10.5194/tc-2023-127
Preprint. Discussion started: 25 August 2023

to accurately capturing SWE change patterns over large areas, especially the accumulation gradient with elevation. The fact that SWE change correlates with elevation also means that practitioners should avoid atmospheric corrections that rely on removing phase vs. elevation relationships, which is common in other InSAR applications. Atmospheric corrections should use atmospheric modeling to generate atmospheric phase delays for corrections. Alternatively, time-series-based analysis, such as small baseline-subset analysis, would also remove temporally random atmospheric effects. However, this will be primarily retrospective after a sufficient winter-time series has been captured and relies on enough temporal coherence between image pairs. Regardless, the atmospheric effects must be considered and corrected for in any practical application of InSAR SWE retrievals. Future work should include interval board measurements over a wide elevation range to identify the correct phase gradient for the InSAR retrieval.

Future work should also focus on how to best use these phase-based SWE change measurements to supplement and expand existing snow monitoring techniques in periods and regions where the technique is most appropriate. These include accumulation periods when non-maritime snowpack tends to be drier and in higher alpine regions with fewer trees and drier snow. Spatially, practitioners could continue to use pre-existing SNOTEL and snow-survey interpolation techniques below treeline where they are more appropriate due to less spatial variability and more uniform elevation gradients in SWE accumulation. In the complex alpine environment above treeline and in regions with less vegetation, pracitioners could apply InSAR retrievals to improve the pre-existing models and capture variability and changes in SWE storage. Temporally, this technique will improve monitoring efforts in the accumulation period when current models struggle to appropriately characterize the patterns and magnitudes of precipitation events, especially in complex terrain with large amounts of wind redistribution. These InSAR phase changes will help constrain those SWE accumulation patterns before taking a less weighted effect later in the season when SWE melt-off is generally well defined by snow models. Integrating InSAR SWE retrievals into existing water monitoring systems will only improve results when appropriately applied, considering the strengths and weaknesses of the technique. Practitioners, considering the limitations mentioned above, could consider InSAR retrievals to be essentially spatially expansive, relevant, remotely-sensed SNOTEL sites.

The locations and setup for the next generation of in situ monitoring stations should also consider the needs and potential of InSAR-based SWE retrievals. Currently, snow monitoring relies on a few heavily instrumented stations to characterize entire basins. Future research should evaluate the utilization of higher densities of simply instrumented in situ stations, capturing only temperature and snow depth, across a smaller region to characterize and validate a small patch of remotely sensed data and modeling results. This smaller region would need to be carefully selected within each study basin to cover the dynamic range of controlling factors including incidence angle, aspect, elevation, and vegetation characteristics. Water forecasters could then rely on that well-validated and calibrated remotely sensed data and model output to forecast across larger regions. Specifically for InSAR phase validation, this could involve capturing SWE change over a range of elevations and aspects to validate atmospheric corrections, confirm the spatial patterns in the InSAR imagery, and remove or correct those affected by low coherence, atmospheric effects, and other biases. Future in situ monitoring sites should consider how their placements and instrumentation complements remote sensing techniques and allows for synergistic combinations with the new tools available to practitioners.

https://doi.org/10.5194/tc-2023-127
Preprint. Discussion started: 25 August 2023

Future research should also evaluate how to use convert intuition based manual checks into automated systems for validating InSAR phase retrievals and ensuring believable spatial trends and magnitude. Most practitioners will have an intuition about likely spatial trends in precipitation that they can initially use to identify image pairs or sub-regions biased by low coherence, unwrapping errors, or biases from snow-wetness within the image. Successful application of this technique will involve finding ways to convert that intuition-based error checking and masking of regions or image pairs into automated checks of the InSAR phase that will control for images with unrealistic results to limit the biasing effects of these errors in any future processing pipelines.

Our study location, in the central mountains of Idaho, has a transitional snow climate with more mid-winter rain and SWE melt to the southwest, and a colder, often deeper snowpack to the northeast, vegetation patterns that are highly aspect and elevation-dependent and range from high-density evergreen to sagebrush to alpine treeless regions. Future work should explore this technique in maritime and continental snowpacks and other vegetation classes, such as tundra or agricultural regions. The SnowEx data provides an opportunity to test this approach in a range of snow climates, and our future work will expand this analysis across the entire SnowEx domain.

We noted significant adverse effects on the correlation between our results and SnowModel SWE changes for periods and regions with wet snow effects. We did not attempt to parameterize or correct, potentially using modeled or elevation-based snow wetness, for these impacts. Future work on retrieval improvements that characterize and account for snow-wetness impacts will be essential to expand this technique into lower-elevations and ablation periods, which will become increasingly important with the more frequently observed mid-winter rain and melt events at greater ranges of elevations.

Finally, a range of other frequencies and SAR techniques exist that could be combined with this technique to improve retrievals and supplement the weaknesses of this technique. Future work should explore snow-depth-based surface topography approaches (SfM, lidar) in periods of wet snow, higher frequency backscatter-based approaches, and snow properties' relationship to coherence and polarimetry.

8 Conclusions

We present a novel comparison of a full winter-season time series of L-band InSAR SWE retrievals against in situ and modeled validation data sets. Our technique shows promise, capturing trends and absolute values of new snow accumulation. We show well matched snow depth and SWE time series from the UAVSAR retrieved values when compared against three SNOTEL stations. Comparisons between in situ observations, captured during the NASA 2020 and 2021 SnowEx campaigns, and UAVSAR retrievals showed high correlation and low RMSEs for snow depth changes (RMSE: <0.1 m and r: 0.80) and SWE change (<0.04 m and r: 0.52). The UAVSAR images also captured orographic trends in new SWE accumulations well when compared to an interval board network setup across a large elevation range for multiple storms. Finally, comparison to SnowModel SWE changes also suggest the L-band InSAR was realistically capturing SWE accumulation with strong correlation between the two (RMSD <0.023 m and r: 0.60) and especially good relationship in regions with limited snow melt and lower vegetation percentages (RMSD <0.013 m and r: 0.72). Using this SnowModel to UAVSAR comparison this study explored the

https://doi.org/10.5194/tc-2023-127
Preprint. Discussion started: 25 August 2023

The Cryosphere
Discussions

controlling factors of this technique's accuracy, including the importance of appropriately applying this technique in regions of relatively-dry snow and lower vegetation percentages based on a comparison to SnowModel SWE change and SWE melt. Overall this study demonstrates the promise of using future L-band InSAR missions for snow water storage monitoring across large regions and time periods.

Code availability. Research code for this study is available at: https://github.com/ZachHoppinen/uavsar-validation.

Author contributions. Conceptualization: SO, ZH, HP. Writing: ZH, RM Analysis: ZH. Model Generation: RM. Funding Acquisition: HPM, CV. Planning: HPM, CV, KE. Editing: ZH, HPM, KE, CV.

Competing interests. CV is a part of the editoral board of The Cyrosphere. The authors have no other competitions of interest.

Acknowledgements. This work was completed with funding from CRREL grant #W913E520C0017 and the NASA Terrestrial Hydrology Program.

https://doi.org/10.5194/tc-2023-127
Preprint. Discussion started: 25 August 2023

References

Hui Li, Zuo Wang, Guangjun He, and Wang Man. Estimating Snow Depth and Snow Water Equivalence Using Repeat-Pass Interferometric SAR in the Northern Piedmont Region of the Tianshan Mountains. *Journal of Sensors*, 2017:1–17, 2017.

Matthew Sturm, Michael A. Goldstein, and Charles Parr. Water and life from snow: A trillion dollar science question. *Water Resources Research*, 53(5):3534–3544, 2017.

Kenneth E. Kunkel, David A. Robinson, Sarah Champion, Xungang Yin, Thomas Estilow, and Rebekah M. Frankson. Trends and Extremes in Northern Hemisphere Snow Characteristics. *Current Climate Change Reports*, 2(2):65–73, 2016.

Judah Cohen, Hengchun Ye, and Justin Jones. Trends and variability in rain-on-snow events. *Geophysical Research Letters*, 42(17):7115–7122, 2015.

Giacomo Strapazzon, Jürg Schweizer, Igor Chiambretti, Monika Brodmann Maeder, Hermann Brugger, and Ken Zafren. Effects of Climate Change on Avalanche Accidents and Survival. *Frontiers in Physiology*, 12:639433, 2021.

F. Dominguez, E. Rivera, D. P. Lettenmaier, and C. L. Castro. Changes in winter precipitation extremes for the western United States under a warmer climate as simulated by regional climate models. *Geophysical Research Letters*, 39(5):n/a–n/a, 2012.

Ben Livneh and Andrew M. Badger. Drought less predictable under declining future snowpack. *Nature Climate Change*, 10(5):452–458, 2020.

Tore Guneriussen, Kjell Arild Hogda, Harald Johnsen, and Inge Lauknes. Insar for Estimation of Changes in Snow Water Equivalent of Dry Snow. *IEEE Transactions on Geoscience and Remote Sensing*, 39(10):2101, 2001.

C. Matzler. Microwave permittivity of dry snow. *IEEE Transactions on Geoscience and Remote Sensing*, 34(2):573–581, 1996.

HP Marshall, Elias Deeb, Rick Forster, Carrie Vuyovich, Kelly Elder, Chris Hiemstra, and Jewell Lund. L-Band InSAR Snow Depth Retrievals from Grand Mesa in NASA SnowEX 2020 Campaign. *Institute of Electrical and Electronics Engineers*, 2021.

Elias J. Deeb, Richard R. Forster, and Douglas L. Kane. Monitoring snowpack evolution using interferometric synthetic aperture radar on the North Slope of Alaska, USA. *International Journal of Remote Sensing*, 32(14):3985–4003, 2011.

Jack Tarricone, Ryan W. Webb, Hans-Peter Marshall, Anne W. Nolin, and Franz J. Meyer. Estimating snow accumulation and ablation with L-band InSAR. *The Cryosphere Discussions*, 2022:1–33, 2022.

J. Jorge Ruiz, J. Lemmetyinen, A. Kontu, R. Tarvainen, J. Pulliainen, R. Vehmas, and J. Praks. Analysis of Snow Coherence Conservation for SWE Retrieval at L-, S-, C-and X-Bands. *2021 IEEE International Geoscience and Remote Sensing Symposium IGARSS*, 00:860–863, 2021.

Thomas Nagler, Helmut Rott, Stefan Scheiblauer, Ludivine Libert, Nico Mölg, Ralf Horn, Jens Fischer, Martin Keller, Alberto Moreira, and Julia Kubanek. Airborne Experiment on Insar Snow Mass Retrieval in Alpine Environment. *IGARSS 2022 - 2022 IEEE International Geoscience and Remote Sensing Symposium*, 00:4549–4552, 2022.

Ethan Greene, Karl Birkeland, Kelly Elder, Ian McCammon, Mark Staples, Don Sharaf, Simon Trautman, and Wendy Wagner. *Snow, Weather, and Avalanches: Observation Guidelines for Avalanche Programs in the United States*. Denver, Colorado, 4 edition, 2022.

Dean G Gesch, Michael J Oimoen, and Samantha Arundel. The National Elevation Dataset. *USGS Publication Warehouse*, 2018.

Suming Jin, Collin Homer, Limin Yang, Patrick Danielson, Jon Dewitz, Congcong Li, Zhe Zhu, George Xian, and Danny Howard. Overall Methodology Design for the United States National Land Cover Database 2016 Products. *Remote Sensing*, 11, 2019.

https://doi.org/10.5194/tc-2023-127
Preprint. Discussion started: 25 August 2023

Peter Potapov, Xinyuan Li, Andres Hernandez-Serna, Alexandra Tyukavina, Matthew C. Hansen, Anil Kommareddy, Amy Pickens, Svetlana Turubanova, Hao Tang, Carlos Edibaldo Silva, John Armston, Ralph Dubayah, J. Bryan Blair, and Michelle Hofton. Mapping global forest canopy height through integration of GEDI and Landsat data. *Remote Sensing of Environment*, 253:112165, 2021.

Scott Hensley, Kevin Wheeler, Greg Sadowy, Cathleen Jones, Scott Shaffer, Howard Zebker, Tim Miller, Brandon Heavey, Ernie Chuang, Roger Chao, Ken Vines, Kouji Nishimoto, Jack Prater, Bruce Carrico, Neil Chamberlain, Joanne Shimada, Marc Simard, Bruce Chapman, Ron Muellerschoen, Charles Le, Thierry Michel, Gary Hamilton, David Robison, Greg Neumann, Robert Meyer, Phil Smith, Jim Granger, Paul Rosen, Dennis Flower, and Robert Smith. THE UAVSAR INSTRUMENT: DESCRIPTION AND FIRST RESULTS. *2008 IEEE Radar Conference*, pages 1–6, 2008.

Paul A. Rosen, Scott Hensley, Kevin Wheeler, Greg Sadowy, Tim Miller, Scott Shaffer, Ron Muellerschoen, Cathleen Jones, Howard Zebker, and Søren Madsen. UAVSAR: A New NASA Airbome SAR System for Science and Technology Research. *2006 IEEE Conference on Radar*, pages 22–29, 2006.

Alexander G. Fore, Bruce D. Chapman, Brian P. Hawkins, Scott Hensley, Cathleen E. Jones, Thierry R. Michel, and Ronald J. Muellerschoen. UAVSAR Polarimetric Calibration. *IEEE Transactions on Geoscience and Remote Sensing*, 53(6):3481–3491, 2015.

Zachary Hoppinen, Jack Tarricone, Naheem Abedisi, and HP Marshall. SnowEx/uavsar_pytools: v0.2.0, 2022.

USDA Natural Resources Conservation Service. SNOwpack TELemetry Network (SNOTEL), 2022.

Glen E. Liston and Kelly Elder. A Distributed Snow-Evolution Modeling System (SnowModel). *Journal of Hydrometeorology*, 7(6):1259–1276, 2006.

Glen Liston, Julienne Stroeve, Samantha Buzzard, Lu Zhou, Robbie Mallett, Andrew Barrett, M. Tschudi, Dr Michel Tsamados, Polona Itkin, and J. Stewart. A Lagrangian Snow-Evolution System for Sea Ice Applications (SnowModel-LG): Part II - Analyses. 125, 10 2020.

L. Carriere. Discover SCU Hardware, 2023.

Collin Homer, Jon Dewitz, Limin Yang, Suming Jin, Patrick Danielson, George Xian, John Coulston, Nate Herold, James Wickham, and Kevin Megown. Completion of the 2011 National Land Cover Database for the Conterminous United States - Representing a Decade of Land Cover Change Information. *Photogrammetric Engineering and Remote Sensing*, 81:346–354, 2015.

Rasim Latifovic, Collin Homer, Rainer Ressl, D.A. Pouliot, S. Hossian, Rene Colditz, Ian Olthof, Giri Chandra, and Arturo Victoria. North American Land Change Monitoring System. pages 303–324, 05 2012.

Roy M. Rasmussen, Fei Chen, Changhai Liu, Kyoko Ikeda, Andreas Prein, Ju-Hye Kim, Timothy Schneider, Aiguo Dai, David Gochis, Aubrey Dugger, Yongxin Zhang, Abby Jaye, Jimy Dudhia, Cinlin He, Michelle Harrold, Lulin Xue, Sisi Chen, Andrew Newman, Erin Dougherty, Ronnie Abolafia-Rozenzweig, Nicholas Lybarger, Roland Viger, Krista A Dunne, Kristen Rasmussen, and Gonzalo Miguez-Macho. Four-kilometer long-term regional hydroclimate reanalysis over the conterminous United States (CONUS), 1979-2020. *Research Data Archive at the National Center for Atmospheric Research, Computational and Information Systems Laboratory*, 2023.

Silvan Leinss, Andreas Wiesmann, Juha Lemmetyinen, and Irena Hajnsek. Snow Water Equivalent of Dry Snow Measured by Differential Interferometry. *IEEE Journal of Selected Topics in Applied Earth Observations and Remote Sensing*, 8(8):3773–3790, 2015.

Hans Hersbach, Bill Bell, Paul Berrisford, Shoji Hirahara, András Horányi, Joaquín Muñoz-Sabater, Julien Nicolas, Carole Peubey, Raluca Radu, Dinand Schepers, Adrian Simmons, Cornel Soci, Saleh Abdalla, Xavier Abellan, Gianpaolo Balsamo, Peter Bechtold, Gionata Biavati, Jean Bidlot, Massimo Bonavita, Giovanna Chiara, Per Dahlgren, Dick Dee, Michail Diamantakis, Rossana Dragani, Johannes Flemming, Richard Forbes, Manuel Fuentes, Alan Geer, Leo Haimberger, Sean Healy, Robin J. Hogan, Elías Hólm, Marta Janisková, Sarah Keeley, Patrick Laloyaux, Philippe Lopez, Cristina Lupu, Gabor Radnoti, Patricia Rosnay, Iryna Rozum, Freja Vamborg, Sebastien

https://doi.org/10.5194/tc-2023-127
Preprint. Discussion started: 25 August 2023

Villaume, and Jean-Noël Thépaut. The ERA5 global reanalysis. *Quarterly Journal of the Royal Meteorological Society*, 146(730):1999–2049, 2020.

M.-P. Doin, C. Lasserre, G. Peltzer, O. Cavalié, and C. Doubre. Corrections of stratified tropospheric delays in SAR interferometry: Validation with global atmospheric models. *Journal of Applied Geophysics*, 69(1):35–50, 2009.

M. Tiuri, A. Sihvola, E. Nyfors, and M. Hallikaiken. The complex dielectric constant of snow at microwave frequencies. *IEEE Journal of Oceanic Engineering*, 9(5):377–382, 1984.

R. Mower, E. D. Gutmann., J. Lundquist, G.E. Liston, and S. Rasmussen. Parallel Implementation of SnowModel (Distributed Snow-Evolution Modeling System). *Geoscientific Model Development*, 2023.